BMC Genomics

RESEARCH Open Access

Partial unidirectional translocation from 5AL to 7BS leads to dense spike in an EMS-induced wheat mutant

Xiaoyu Zhang[1†], Yongfa Wang[1†], Yongming Chen[1], Yazhou Li[2], Kai Guo[1], Jin Xu[1], Panfeng Guan[1], Tianyu Lan[1], Mingming Xin[1], Zhaorong Hu[1], Weilong Guo[1], Yingyin Yao[1], Zhongfu Ni[1], Qixin Sun[1], Ming Hao[2*] and Huiru Peng[1*]

Abstract

Background As the inflorescence of wheat, spike architecture largely determines grain productivity. Dissecting the genetic basis for the spike morphology of wheat can contribute to the designation of ideal spike morphology to improve grain production.

Results The present study characterizes a *dense spike1* (*ds1*) mutant, derived from Nongda3753, induced by EMS treatment, which exhibits a dense spike and reduced plant height. Through bulked segregant analysis sequencing (BSA-Seq) of two segregating populations, *ds1* was mapped to the short arm of chromosome 7B. Further genotypic and phenotypic analyses of the residual heterozygous lines from F_3 to F_6 of Yong3002×*ds1* revealed that there was a 0-135 Mb deletion in chromosome 7B associated with the dense spike phenotype. The reads count analysis of the two bulks in BSA-Seq, along with the cytological analysis of *ds1*, ND3753, NIL-*ds1* and NIL-Y3002, confirmed that the partial unidirectional translocation of 5AL (543–713 Mb) to 7BS (0-135 Mb) exists in *ds1*. This translocation led to an increase in both copy number and expression of the *Q* gene, which is one of the reasons for the dense spike phenotype observed in *ds1*.

Conclusion Partial unidirectional translocation from 5AL to 7BS was identified in the EMS-induced mutant *ds1*, which exhibits dense spike phenotype. This research illustrates the effect of one chromosome structure variation on wheat spike morphology, and provides new materials with several chromosome structure variations for future wheat breeding.

Keywords *Triticum aestivum* L., EMS-induced mutant, Chromosomal translocation, Dense spike, *Q* gene

†Xiaoyu Zhang and Yongfa Wang contributed equally to this work.

*Correspondence:
Ming Hao
haomingluo@foxmail.com
Huiru Peng
penghuiru@cau.edu.cn; penghuiru1452@163.com
[1]Frontiers Science Center for Molecular Design Breeding, Key Laboratory of Crop Heterosis and Utilization, Beijing Key Laboratory of Crop Genetic Improvement, China Agricultural University, Beijing 100193, China
[2]Triticeae Research Institute, Sichuan Agricultural University, Chengdu, Sichuan 611130, China

Introduction

Common wheat (*Triticum aestivum* L.) is cultivated worldwide and accounts for approximately 20% of the daily calorie intake of humans [1]. To sustainably support the ever-increasing world population and farming profitability, wheat productivity must increase under fewer production hectares. The spike or inflorescence is the most significant part of cereal crops because of its capacity to produce carbohydrate-rich grains that are harvested for food, fiber and feed [2]. Modifying spikes to increase grain capacity is important for wheat grain production. Spike morphology is a crucial agronomic characteristic that depends on the spike length and spikelet number and is significantly correlated with grain number and yield in wheat [3]. Therefore, dissecting the genetic basis for the spike morphology of wheat can contribute to the designation of ideal spike morphology to improve grain production.

Generally, the spike types of wheat species can be divided into three main morphological variants: compact, normal and speltoid [3]. A compact spike shape was identified in club wheat (*Triticum compactum* Host.), with short, dense spikes and fewer spikelets per spike, which is attributable to a dominant locus *C* localized on chromosome 2D close to the centromere [4–6]. However, at the molecular level, the *C* locus remain uncharacterized, mainly because of their location in proximal segments of chromosomes regions with reduced levels of recombination. The essential domestication gene *Q* exists on the long arm of chromosome 5A (5AL), has been studied for decades owing to its important role in the regulation of spike morphology and other domestication-related characteristics in wheat [7–12]. The normal spike shape was identified in cultivated wheat species that carry the domesticated *Q* allele, which is responsible for the relatively short, square-headed, parallel-sided spikes. The speltoid spike has a pyramidal inflorescence shape featuring an elongated rachis, and tenacious glumes exist in spelt (*T. aestivum* ssp. *spelta*), which is considered to have the primitive *q* allele [13]. There are two main differences between the sequences of *q* and *Q* alleles: (1) a nonsynonymous G-to-A substitution, which results in an amino acid substitution at the position 329 (Val/Ile), and (2) a neutral single nucleotide polymorphism (SNP) at the binding site of microRNA172 (miR172) within exon 10 (T/C) [13]. The presence of 329Ile is predicted to increase the level of *Q* homodimers, resulting in the self-upregulation of *Q* transcription [14]. The mutation at the miR172 binding site of the *Q* allele leads to less effective targeting by the miRNA, which triggers an increase in the expression of *Q* [15]. Through miRNA mimic targeting, the miR172 activity would be inhibited, then the transcription of *Q* gene would elevate, resulting in a compact spike phenotype [16], which suggests that the *Q* gene influences spike shape in a dosage-dependent manner. In addition, the cytogenetic experiments also indicated that the *Q* gene had a dosage effect on spike morphology. In the *T. aestivum* cv. Chinese Spring (CS) background, plants with different copy numbers of the *Q* allele, such as nullisomic, monosomic, disomic, trisomic, and tetrasomic for chromosome 5A, display the speltiod, semi-speltoid, square, subcompactoid, and compactoid spikes, respectively [7].

Translocations represent a significant type of genomic structural variation with DNA regions that have altered locations, which have important functional and evolutionary impacts on species [17]. These chromosomal rearrangements may occur in the homologous recombination pathway at meiosis due to compromised meiotic fidelity and can be detected by fluorescence in situ hybridization (FISH) [18, 19]. In wheat, chromosome translocations are prevalent and play important roles in genetic adaptation and genome evolution. For example, the genes located within the translocation region are suppressed in recombination, which results in highly independent genome evolution between derived and ancestral arrangements [20]. This provides opportunities for shaping novel genotypes and phenotypes, and driving the divergence and speciation we observe today [21]. In addition to their evolutionary significance, several studies on translocations have focus on crop breeding applications [22, 23]. Many natural or artificial translocations have been reported to be associated with important agronomic traits [22, 24, 25], and several wheat-alien translocations, such as T6VS•6AL and T1RS•1BL have already been identified and used in wheat breeding programs [26, 27]. By reorganizing large regulatory domains and altering epigenetic or genetic environments near the translocated breakpoints, translocations can influence gene expression related to important agronomic and adaptive traits [28, 29]. Therefore, perceiving the frequency and distribution of beneficial translocations in populations is important for breeders to enhance and control the inheritance of specific traits in the breeding process.

This study identified an ethyl methane sulfonate (EMS)-induced dense spike mutant *dense spike1* (*ds1*), which has decreased plant height and increased spike density. Through map-based cloning, sequence comparison, cytological and expression analyses, a partial unidirectional translocation from 5AL to the short arm of chromosome 7B (7BS) was demonstrated in *ds1*, resulting in an increase in the copy number and expression of the *Q* gene, which is one of the reasons for the mutant phenotype. This research illustrates the effect of the chromosome structure variation (CSV) on wheat spike morphology, and provides new insights into the potential genetic mechanisms leading to the CSVs in an EMS-induced mutant.

Materials and methods

Wheat materials and growth conditions

The mutant (*ds1*) with increased spike density and shortened plant height was isolated from 0.4% EMS-treated common wheat (*Triticum aestivum* L.) cultivar "Nongda3753 (ND3753)". The *ds1* mutant was crossed with ND3753 and with the spring hexaploid wheat Yong3002 (Y3002) separately to produce two F_2 populations. The cross of *ds1*×Y3002 was used for fine-mapping by selecting the plants with different heterozygous segments at each generation. The important line C2 was selected at $F_{2:3}$ to generate $F_{3:4}$. Through marker screening and phenotype evaluation of the recombinants from the F_4 to F_6 generations, the homozygous lines of the segregating plants with the smallest heterozygosity interval were selected to develop the corresponding near-isogenic lines (NILs) in the $F_{6:7}$ generations. NIL-Y3002 contains the normal 7B and 5A chromosomes, but the NIL-*ds1* contains the unbalanced translocation between 7B and 5A chromosomes. The F_2 populations of ND3753×*ds1*, Y3002×*ds1* and the segregating families from the F_3 to F_6 generations were planted at the China Agriculture University Experimental Station (Beijing, China) from 2017 to 2022.

Phenotypic analysis

The spike morphologies of individual plants were classified as A (normal spike), H (medium), or B (dense spike). The phenotypes of imported recombinant plants were determined by testing their progeny during the subsequent growing season.

BSA-Seq (bulked segregant analysis sequencing) analysis

The whole-genome sequencing data of the bulks were processed and filtered by fastp with the default parameters [30]. The remaining high-quality clean reads were then mapped to the CS wheat reference genome [31], IWGSC RefSeq v2.1 [32], using BWA-MEM v0.7.15 [33]. Picard v2.9.0 software (http://broadinstitute.github.io/picard/) was further used to remove the potential PCR duplicates. SNPs and InDels were called by the HaplotypeCaller module of GATK v3.8 in GVCF mode [34]. The GenotypeGVCFs module of GATK v3.8 was subsequently used to perform the joint call [34]. The SNPs were initially filtered via the GATK VariantFiltration function with the parameter "–filterExpression QD < 2.0 || FS > 60.0 || MQRankSum < −12.5 || ReadPosRankSum < −8.0 || SOR > 3.0 || MQ < 40.0 || DP < 3." The filtering settings for `InDels were "QD < 2.0 || FS > 200.0 || ReadPosRankSum < −20.0 || DP < 3." Variants that did not fit the criteria were excluded. A valid variant site was further defined by having only two called alleles by vcftools v0.1.13 [35]. The identified variants were annotated using the SnpEff tool [36]. The AFD between the bulks for each variant was subsequently calculated using the following formulas: n_L = n_AL + n_aL, n_D = n_AD + n_aD, AFD = |n_aL/n_L - n_aD/n_D |. A representative allele of SNP was identified among the two pools. L and D represent pools of normal spike (L) and dense spike (D), respectively. n represents the number of reads supporting the allele. Using a 1-Mb window size, the average AFD in each window was calculated and visualized by sliding the window. Variants with an AFD > 0.5 were considered significantly associated variants. Additionally, we calculated the average value of read coverage in each 1-Mb window and divided it by the average value of reads coverage in all windows to determine genomic structural variations.

Genetic mapping

On the basis of the candidate intervals identified via BSA-Seq analysis, we developed insertion/deletion (InDel) markers to genotype the F_2 to F_6 populations of Y3002×*ds1*. The PCR procedures were set as follows: 1 cycle of 94℃ for 5 min; 35 cycles of 94 ℃ for 30s, 60℃ for 30s, and 72℃ for 30s; and final extension with 72℃ 5 min. Electrophoresis with 10% nondenaturing polyacrylamide gel or 1% agarose was used to separate the PCR products [37]. Through genotypic and phenotypic analyses of residual heterozygous lines, the candidate interval of *ds1* was further narrowed to the region between marker D130 and the telomere of the terminus of 7BS. The primers used for fine-mapping are listed in Table S3.

Cloning of *Q* gene sequence

Genomic DNAs were extracted from the young leaves of ND3753 and *ds1* using the cetyltrimethylammonium bromide (CTAB) method [38]. The specific primer for cloning *Q* gene was designed based on the reference genome downloaded from the WheatOmics1.0 tools JBrowse [39], which was listed in Table S3. The PCR procedures consisted of a 5 min denaturation at 98 ℃, followed by 35 cycles of 98 ℃/10 s, 60 ℃/15 s and 68 ℃/2 mins 30s, with a final extension of 68 ℃/5 mins. Tks Gflex DNA polymerase (Takara Bio Inc., Beijing, China) was used to amplify *Q* gene in *ds1* and ND3753. DNAMAN v9 was used for sequence alignment.

RNA extraction, cDNA preparation, and quantitative RT-PCR (RT-qPCR)

Young spikes of ND3753 and *ds1* were sampled at Waddington scales W4, W5, and W6 [40], with three plants per biological replicate for RNA extraction. Total RNA was extracted using the standard TRIzol RNA isolation protocol (Thermo Fisher Scientific, Waltham, MA, USA) following the manufacturer's instructions. A reverse transcription kit (R223, Vazyme, Nanjing, China) was used to remove gDNA, and first-strand cDNA was synthesized.

RT-qPCR was performed using SYBR Green PCR Master Mix (Q121, Vazyme, Nanjing, China) on a CFX96 Real-Time PCR Detection System (CFX96, Bio-Rad Laboratories, Hercules, California, USA). The procedures of RT-qPCR were set as follows: Pre-degeneration (95 ℃, 5 min); followed by 40 cycles all of degeneration (95 ℃, 10 s), annealing (60 ℃, 10 s), extension (72 ℃ 15 s); and a melting curve from 65 °C to 95 °C (0.1 °C/s). The wheat gene *β*-ACTIN was used as a reference gene. The primers used are listed in Table S3. Relative expression levels were calculated using the ΔΔCT (DDCT) method [41].

Cytological analysis

ND-FISH analysis was performed according to the methods described by Tang et al. [42]. The oligonucleotides probes used for ND-FISH were Oligo-pTa-535 (5´-AAAA ACTTGACGCACGTCACGTACAAATTGGACAAACT CTTTCGGAGTATCAGGGTTTC) and Oligo-pSc119.2 (5´- CCGTTTTGTGGACTATTACTCACCGCTTTG GGGTCCCATAGCTAT) [43]. The 5´ of probes were labeled with 6-FAM and Tamra respectively, and these probes were synthesized by Sangon Biotech Co., Ltd. (Shanghai, China). Slides prepared from the same root tip were analyzed by multicolor GISH on the basis of the methods of Han et al. [44]. The genomic DNA of *Aegilops tauschii* (D genome; 200 ng/μl) and *Triticum urartu* (A genome; 200 ng/μl) were labelled with ATTO-488 and ATTO-550 by nick-translation by ATTO NT Labelling Kit (Jena Bioscience, Germany) as probes. *Aegilops speltoides* (S genome) DNA (3800 ng/μl) was used as a blocker (D: A:S = 1.3:1:180). 4',6-diamidino2-phenylindole (DAPI) was used for chromosome preparation counterstaining in Vectashield (Vector Laboratories, Burlingame, USA). The hybridization signals were visualized and captured via an Olympus BX-63 epifluorescence microscope equipped with a Photometric SenSys DP70 CCD camera (Olympus, Tokyo, Japan). The Photoshop v.7.1 (Adobe Systems Inc., San Jose, CA, USA) was used for raw image processing.

Copy number variation determination

To test the copy number of *Q* gene in the *ds1*, ND3753, Y3002 and $F_{6:7}$ progenies with a dense spike phenotype, TaqMan copy number assays were performed. The wheat *CONSTANS2* gene (*TaCO2*) was used as a single-copy control [45, 46]. Specific primers and probes were designed on the basis of *Q* and *TaCO2* sequences (Table S3). Amplification and fluorescence detection were performed using AceQ® U^+ Probe Master Mix (Q113, Vazyme, Nanjing, China) with a CFX96 real-time PCR system (CFX96, Bio-Rad Laboratories, Hercules, California, USA). The PCR parameters were set as follows: 1 cycle of 95℃ for 5 min; 45 cycles of 95 ℃ for 10s, 60 ℃ for 30s; a melting curve from 65 °C to 95 °C (0.1 °C/s). Delta Cq values were calculated and used to determine the copy number of the *Q* gene. Six plants of each genotype were used to calculated the average values in the analysis.

Statistical analyses

GraphPad Prism 8.0 (GraphPad Software, Boston, MA, USA) was used for data analysis and plotting. Chi-square (χ^2) tests for goodness-of-fit were used to test whether the segregation ratios of dense spikes and normal spikes fit the Mendelian segregation.

Results

Phenotypic characterization of the dense spike mutant *ds1*

A common wheat mutant, *ds1*, with dwarf and increased spike density phenotypes (Fig. 1a), was isolated from the EMS-treated wheat cultivar "ND3753". In contrast to the wild-type ND3753 plants, the *ds1* plants presented decreased internode length, especially the peduncle length, causing a 46.2% of reduction in plant height (Fig. 1a and b). In addition, the average spike length of *ds1* decreased by 51.6%, and the average spikelet number was reduced slightly in *ds1* (14.3) compared with ND3753 (16.2), which resulted in a higher spike density of 4.05 in *ds1* than that in ND3753 (2.21) (Fig. 1b).

Genetic analysis of *ds1*

When the *ds1* mutant was crossed with its wild-type ND3753, the F_1 plants exhibited increased spike density and a dwarf phenotype, which was similar to that of *ds1* (Fig. 1a), indicating that the *ds1* mutant has dominant effects. Within the F_2 population (ND3753×*ds1*), the spike density of individuals ranged from 1.84 to 5, and exhibited a bimodal pattern of segregation. The spike length also exhibited a bimodal pattern, whereas the plant height and peduncle length were continuously distributed with no regularity, suggesting these traits might be influenced by more than one gene (Fig. 1c). Moreover, only 639 out of the 1,030 plants displayed compact spikes in the ND3753×*ds1* F_2 population. The X^2-test revealed a significantly distorted segregation for spike density from the 3:1 Mendel's ratio (Table S1), with dramatically fewer compact spike plants. Considering that spike density is a clear segregating phenotype and strongly correlated with the plant height and spike length (Table S2), we decided to use spike morphology as the target trait for mapping the causative gene *ds1*, which pleiotropically affects plant height and spike length.

ds1 was mapped to chromosome 7B by BSA-Seq

BSA-Seq analysis is a rapid strategy to map genes of interest based on comparisons with traditional genetic linkage mapping [47]. In this study, the BSA-Seq was performed in the ND3753×*ds1* F_2 population. Two bulks

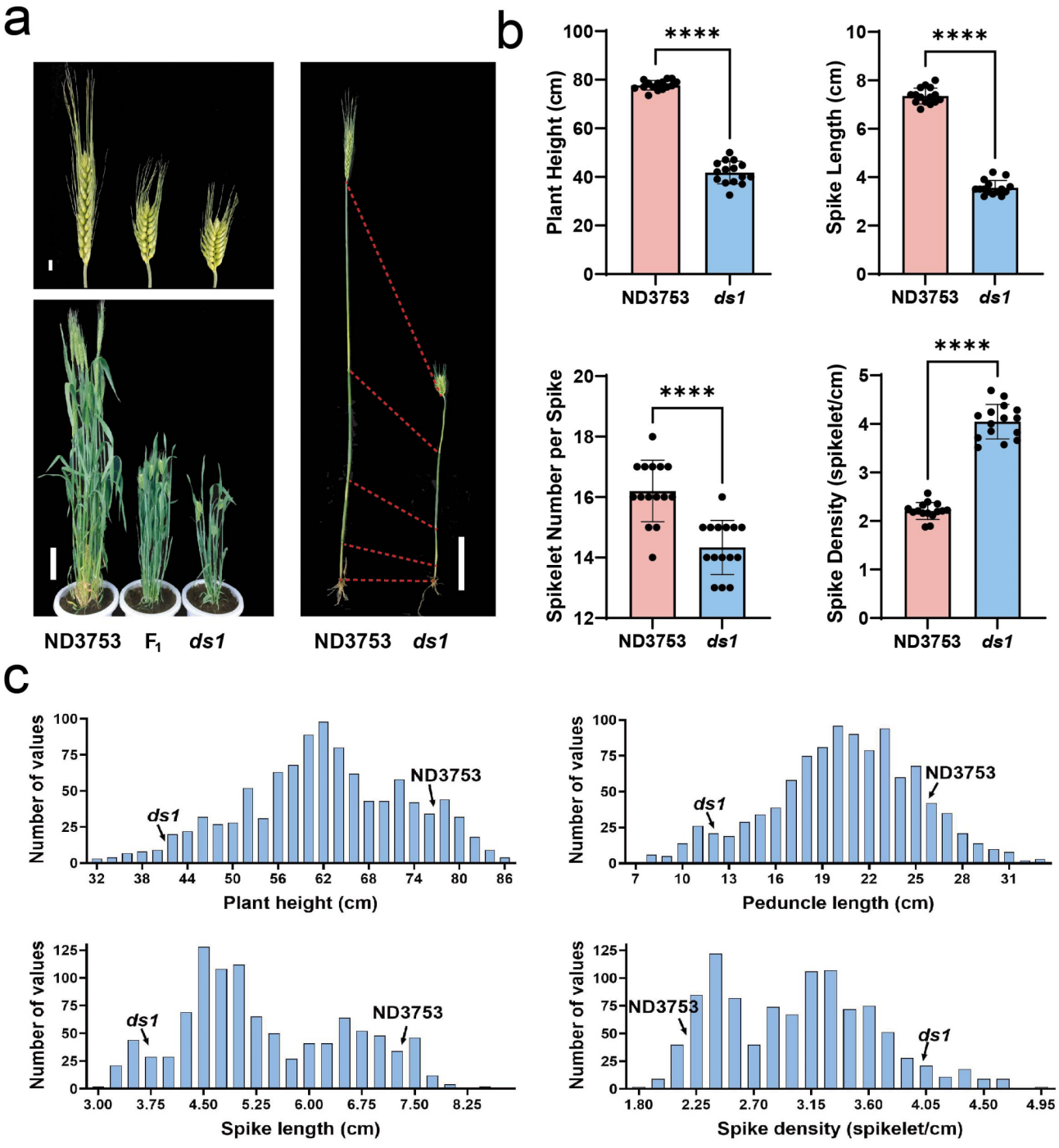

Fig. 1 Phenotypic analysis of the *dense spike1* (*ds1*). (**a**) Phenotypes of ND3753, F_1 and *ds1* at the heading stage. The scale bar in the left top was 1 cm, in the left below and the right were 10 cm. (**b**) The plant heights, spike lengths, spikelet number per spikes and spike densities of ND3753 and *ds1*. The data are presented as the mean, and the error bars indicate the SD.**** indicates significant differences at the 0.0001 level (Student's *t*-test). (**c**) Distribution of plant height, peduncle length, spike length and spike density in the segregating ND3753×*ds1* F_2 population ($n = 1030$)

corresponding to normal spike and dense spike phenotypes were sequenced by next-generation sequencing technology. To identify the chromosomal regions associated with dense spike phenotypes, we calculated the AFD between normal-spike- and dense-spike-bulks in 1 Mb sliding windows (with a step size of 100 kb) and scanned for variations-enriched regions. The result showed that the telomeric region on short arm of chromosome 5D and 7BS both presented significant peaks (Fig. 2a). To further verify the chromosomal location of *ds1*, we

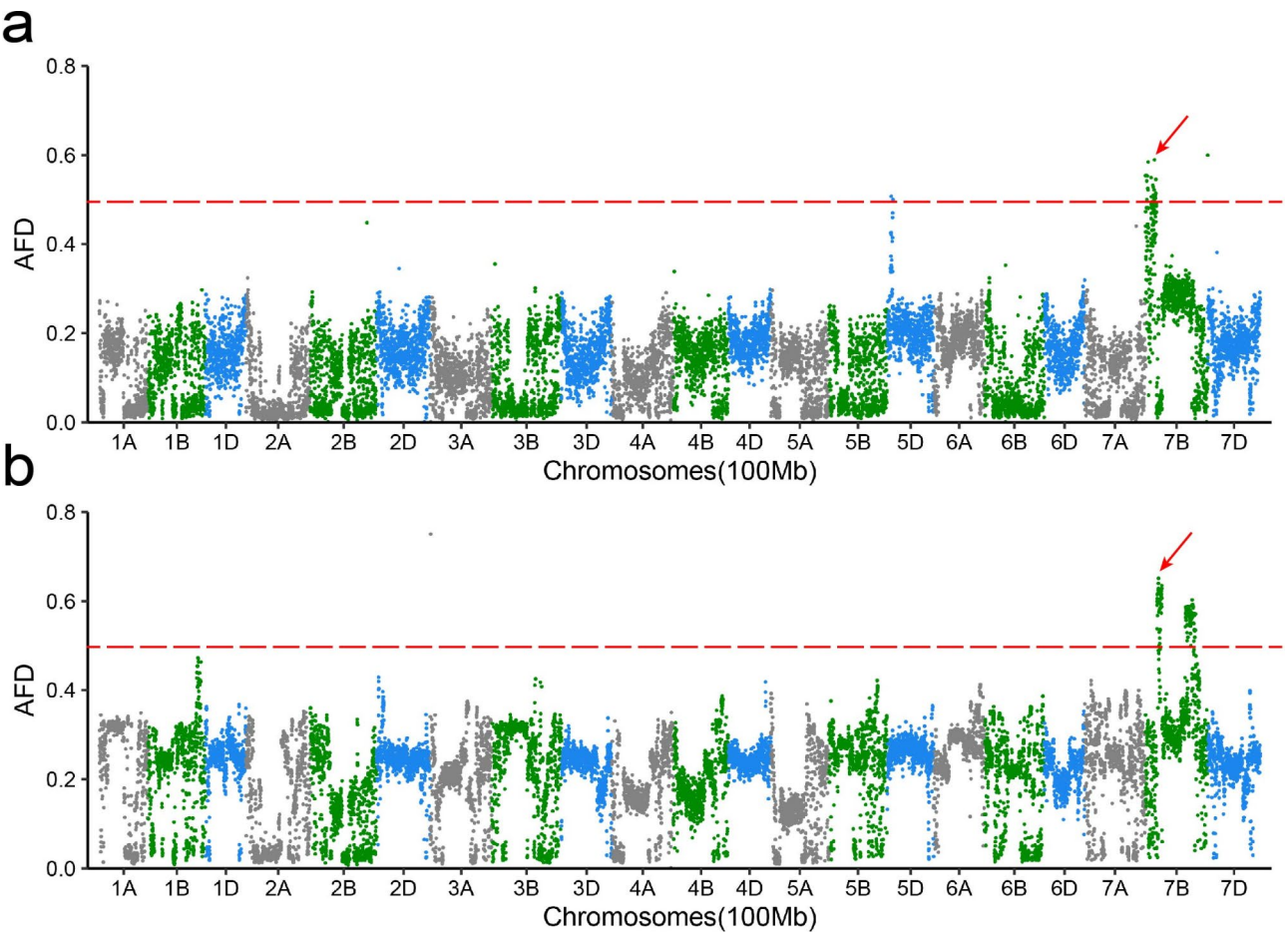

Fig. 2 The BSA-Seq analysis of two F_2 populations. (**a**) Allele frequency difference (AFD) graph from BSA-Seq analysis of the two bulks in ND3753×*ds1* population. (**b**) Allele frequency difference (AFD) graph from BSA-Seq analysis of the two bulks in Y3002×*ds1* population. The horizontal red dashed lines indicate the threshold (0.5) at the overall significance level of $P < 0.05$ and the red arrows indicate the enrich variations peaks of chromosome 7B

also crossed *ds1* with the spring wheat variety Y3002, and performed BSA-Seq analysis of the F_2 population of the Y3002×*ds1*. Significant signals were specifically detected on chromosome 7B rather than chromosome 5D (Fig. 2b). Taken together, the results indicate that the causal region for the *ds1* phenotype is located on the chromosome 7BS.

Fine mapping of *ds1*

Considering the high diversity between Y3002 and *ds1* in terms of genetic background and spring growth habit of Y3002, we used the Y3002×*ds1* population to fine map the candidate gene *ds1*. F_2 individuals were identified with the InDel markers D153 and D552, which are located on chromosome 7BS and the long arm of chromosome 7B (7BL), respectively. We identified three types of recombinants and six additional markers were developed to genotype these recombinants. Their F_3 families were planted to verify the phenotype of the F_2 individuals, which further located *ds1* between the D58.7 and D252 markers (Fig. 3a). Six additional indel markers were developed to characterize the genotype of C2, which narrowed the location of *ds1* to the interval from markers D130 to D202 (72-Mb physical region) (Fig. 3b). Next, we used the InDel markers D138 and D183, which lie in the heterozygous interval, to screen a larger population of 1,976 plants derived from the selfing of the residual heterozygous lines. Four recombination events were identified between D138 and D183 based on the spike morphologies and genotypes of these recombinants, which delimited the *ds1* locus to a 16-Mb interval (Fig. 3c). In addition, we noticed that the recombinant R4 and its $F_{4:5}$ family all showed a dense spike phenotype, indicating that they were all homozygous at the *ds1* locus. Surprisingly, we could not amplify the marker D130 located on the 7BS in these R4 individuals and its $F_{4:5}$ family (Fig. 3d).

Therefore, we further developed three 7BS-specific markers, D3.79, D4.18 and D105, located in the 0-135 Mb region to check the recombinant R4 and its derived progenies. Similarly, none of these markers could be amplified in these individuals (Fig. S1a), revealing that there

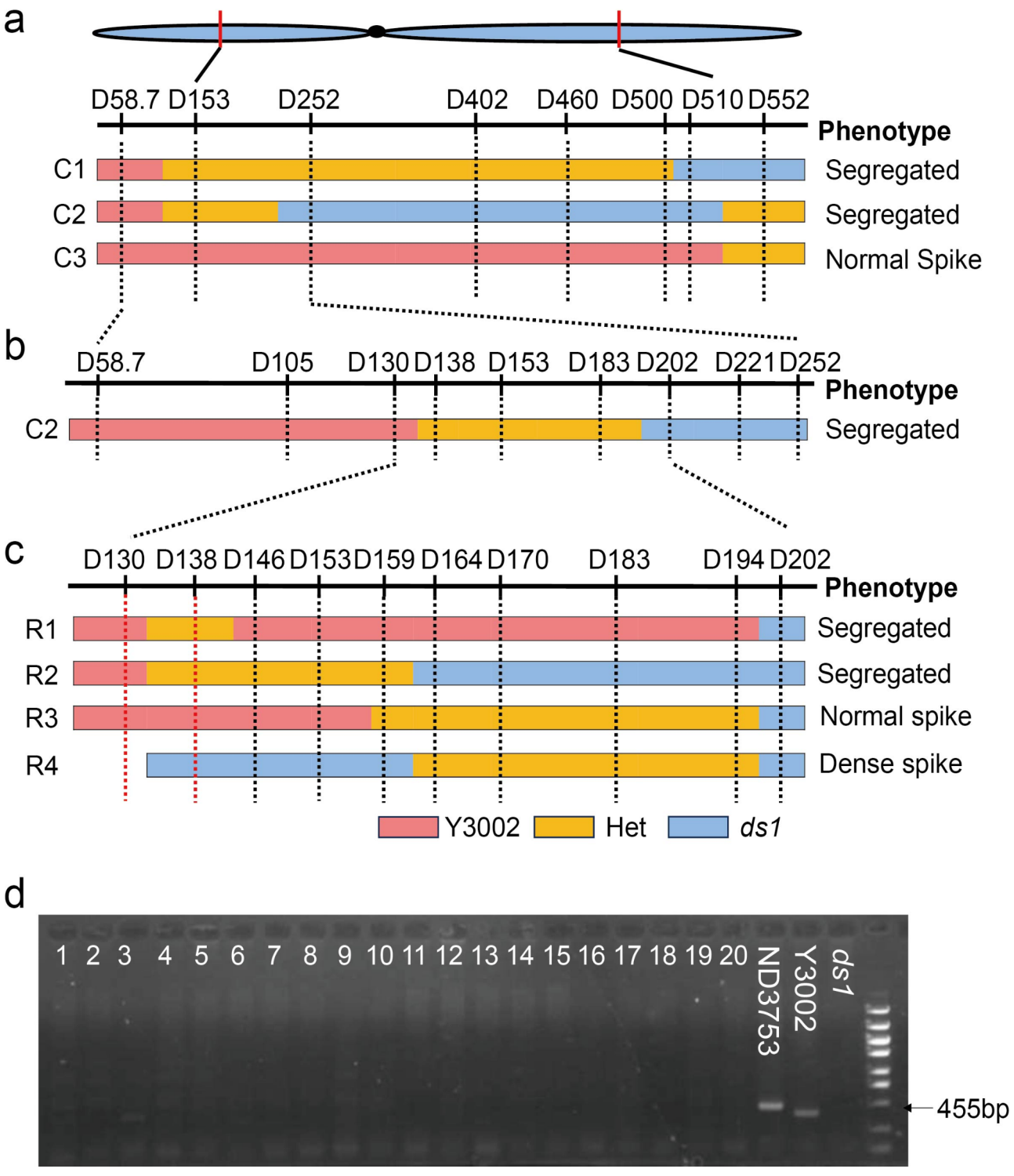

Fig. 3 Fine-mapping of the *ds1* gene. (**a**) Marker screening identified three recombinants between D153 and D510 in the F_2 population of Y3002×*ds1* including 268 individuals. Genotypes of the three representative recombinant plants were shown. (**b**) Additional six InDel markers were developed to characterize the genotype of the recombinant C2. (**c**) Genotypes of four recombinants between D138 and D183. An important recombinant R4 with dense spike but the marker D130 cannot amplified were shown. pink, blue and orange bars represented the genotypes from Y3002, *ds1* and heterozygous plants. The recombination break point was set in the middle between neighboring markers. (**d**) Amplification for marker D130 in 20 progenies from R4. Arrows indicate polymorphic DNA bands. M, DNA Ladder 5000

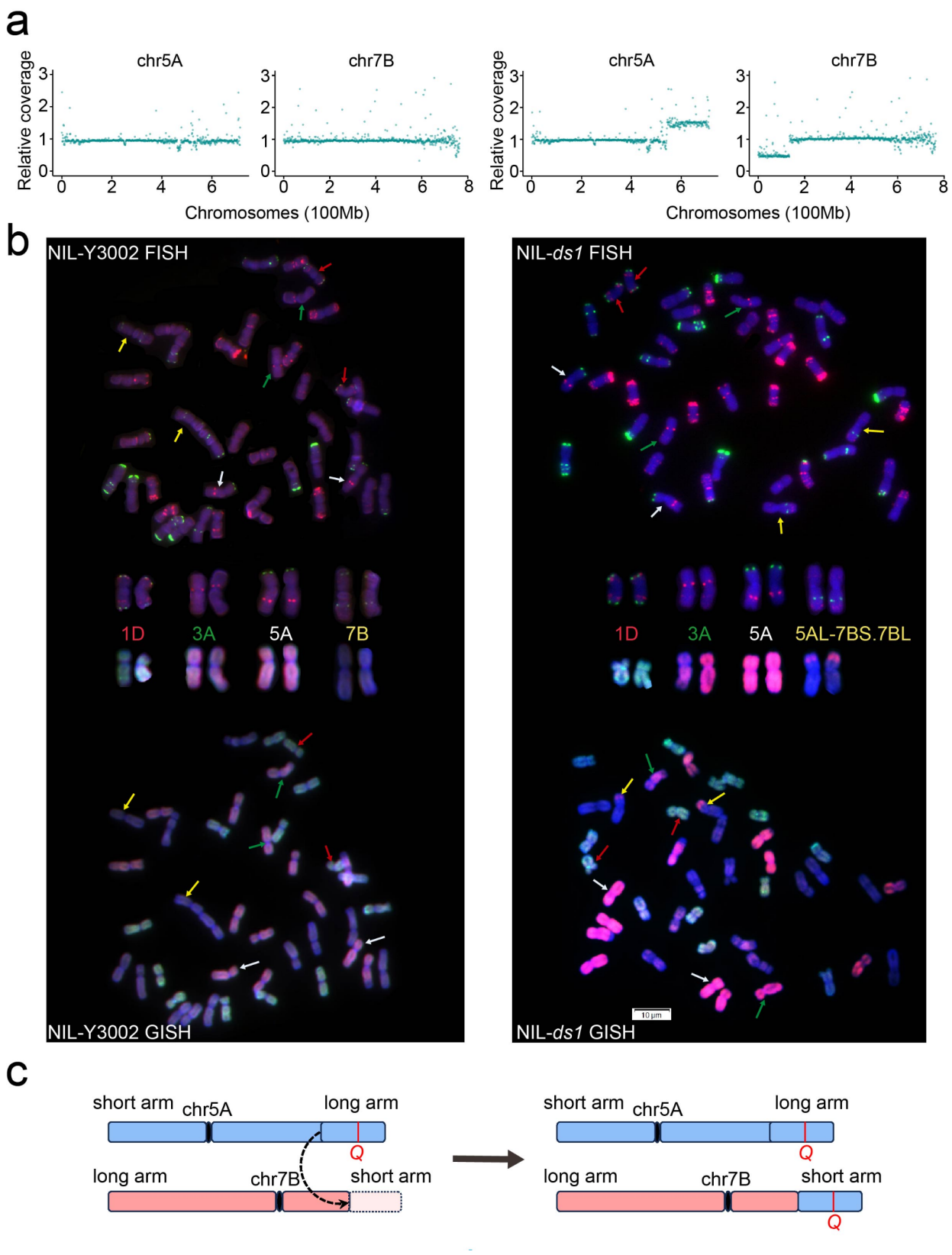

Fig. 4 (See legend on next page.)

(See figure on previous page.)

Fig. 4 The UT (5AL; 7BS) in NIL-*ds1* derived from Y3002×*ds1* population. (**a**) The 5A and 7B chromosomes relative reads coverages of normal-spike bulk (left) and dense-spike bulk (right) from the Y3002 and *ds1* population. (**b**) Fluorescence in situ hybridization/genomic in situ hybridization illustration of NIL-Y3002 and NIL-*ds1* from Y3002×*ds1* $F_{6:7}$ population. The different colorful arrow bar: red, green, white and yellow point to chromosomes 1D, 3A, 5A and 7B respectively. There only has UT (5AL; 7BS) in NIL-*ds1*. UT, unidirectional translocation. (**c**) Schematic of the partial unidirectional translocation between chromosomes 5AL and 7BS. The left chart shows that the part of 7BS chromosome was missing and the part of 5AL chromosome was duplicated and translocated into chromosome 7BS. The right chart shows the formed UT (5AL; 7BS) in new chromosome 7B of *ds1*. Blue chromosome model represents 5A, Pink one represents 7B, light pink represents the missing chromosome segment on 7BS

might be a large fragment deletion on the terminus of chromosome 7BS in the recombinant R4 and its derived progenies. Furthermore, we selected all the $F_{4:5}$ progenies derived from other important recombinants for fine-mapping. We found that the marker D130 was absent in the individuals with the compact spike phenotype (Fig. S1b), whereas target DNA bands were successfully amplified in those individuals with the normal-spike phenotype. Taken together, the co-segregation of the phenotypes with markers on 7BS (0-130 Mb) revealed that the ~130-Mb terminal deletion of chromosome 7BS may be associated with the dense spike phenotype in the mutant *ds1*.

Unidirectional translocation from 5AL to 7BS affects the dosage of *Q* gene, leads to dense spike in the mutant *ds1*

To verify the structural chromosome variation of the mutant *ds1*, we analyzed the relative coverage of reads based on the resequencing data of the normal- and dense-spike pools in the Y3002×*ds1* and ND3753×*ds1* F_2 populations. We found that the coverage of reads on 7BS (0-135 Mb) in the dense-spike pools was very low, which was consistent with the identification of terminal deletions from the InDel markers located on 7BS (0-135 Mb) (Fig. 4a and S2a). Interestingly, we also found that the coverage of reads from 543 to 713 Mb on 5AL in the dense-spike pool was probably twice as much as that in normal-spike pool (Fig. 4a and S2a), indicating that there may be a segmental chromosome duplication in the terminal region of 5AL (543–713 Mb). In addition, the fragment length of the deletion on 7BS was approximately equal to the terminal duplication of 5AL, which prompted us to speculate that there might be an additional chromosome terminus of 5AL translocated to the 7BS.

To further confirm this assumption, FISH and genomic in situ hybridization (GISH) analyses were conducted on ND3753, *ds1*, NIL-Y3002, and NIL-*ds1*" (Fig. S3). The results revealed that a partial unidirectional translocation from 5AL to 7BS, designated as UT (5AL; 7BS), existed in the *ds1* and NIL-*ds1*, in which a part of chromosome segment of the 7BS terminus has been replaced by the terminal parts of the 5AL (Fig. 4b and S2b). Moreover, we also detected a reciprocal translocation between chromosomes 1D and 3A, designated as RT (1DL; 3AS), which resulted in new 1DL-3AS•3AL and 1DS•1DL-3AS chromosomes in *ds1* (Fig. S2b), whereas they were not present in the NIL-*ds1* (Fig. 4b).

Notably, the wheat domestication gene *Q* was located on the 5AL terminus, and the phenotype of the increased copy number or expression of *Q* gene was very similar to that of *ds1* [7, 14, 48, 49]. Therefore, we speculated that the duplicated chromosome segment of 5AL contained the *Q* gene, which may lead to an increase in the copy number of the *Q* gene and thus affect spike morphology in the *ds1*. To investigate the copy number of the *Q* gene, we conducted a TaqMan qPCR assay in ND3753, *ds1*, NIL-Y3002 and NIL-*ds1*. The duplication of *Q* was confirmed in *ds1* and NIL-*ds1*, while ND3753 and NIL-Y3002 carried a single copy of the *Q* gene (Fig. 5a). In addition, the expression of the *Q* gene was greater in the spikes of *ds1* than in those of ND3753 at different development phases (Fig. 5b). Overall, we concluded that the partial unidirectional translocation of 7BS and 5AL effects the copy number and expression of the *Q* gene, which is one of the reasons for the dense spike phenotype in mutant *ds1* (Fig. 4c).

Discussion

The putative mechanism responsible for chromosome structure variations in *ds1*

EMS is a chemical mutagen that mainly induces base pair substitutions and low levels of chromosome breaks in plant genomes [50]. It has been reported that EMS treatment can influence DNA methylation processes and thus impact genomic stability [51]. The higher the EMS concentration is, the more chromosome aberrations are observed in cowpea [52]. It has been reported that the EMS induced partial of chromosome 2D deletion in wheat [53], which indicated that EMS may led the chromosome structure variations in *ds1* directly.

However, the large chromosome structural variations, such as RT and UT, should be rare in one mutant event induced by EMS in crops [54].Considering the low frequency of chromosome structural variation induced by EMS, we speculated that the chromosome translocations in the mutant *ds1* might be induced by mutated gene(s) involved in chromosome stability, chromosome breakage and rearrangement, or meiotic chromosome pairing, which needs further study. The mutated gene(s) may reduce meiotic fidelity, causing nonhomologous chromosomes to pair and recombine, thus resulting in chromosome translocations in *ds1* (Fig. 6). In this case,

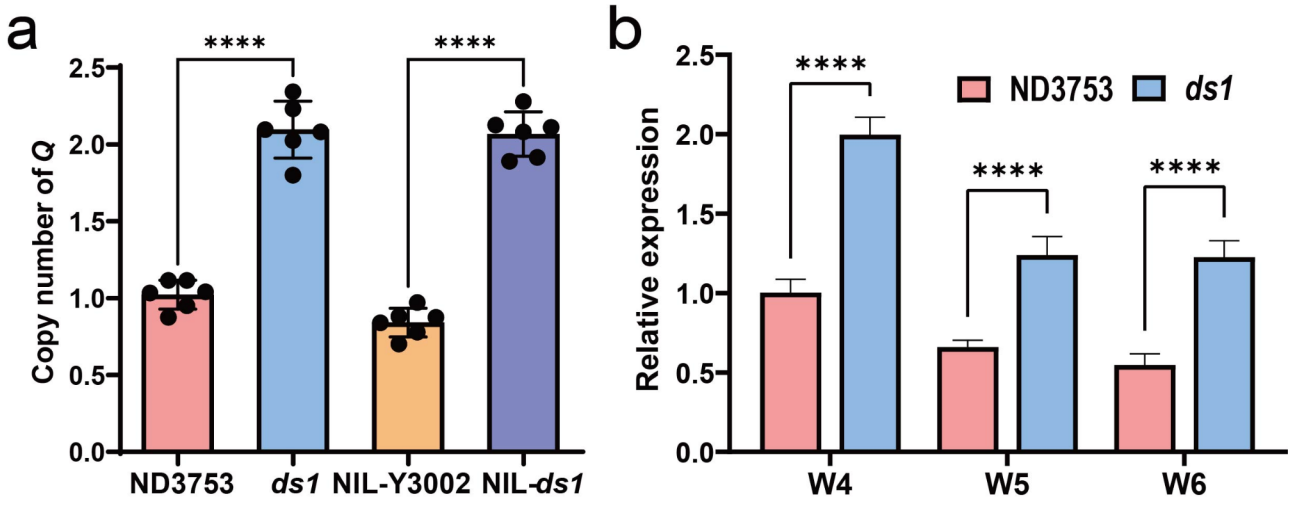

Fig. 5 The copy number and expression analysis of *Q* gene in *ds1*. (**a**) TaqMan estimates of the *Q* gene copy number in ND3753, *ds1*, NIL-Y3002 and NIL-*ds1*; Copy number was estimated from the *Q/TaCO2* signal ratio and were normalized to the ND3753 control. (**b**) The relative expression levels of *Q* from stages W4 to W6 were measured by RT-qPCR. The data are presented as the mean, and the error bars indicate the SD.**** indicates significant differences at the 0.0001 level (Student's *t*-test)

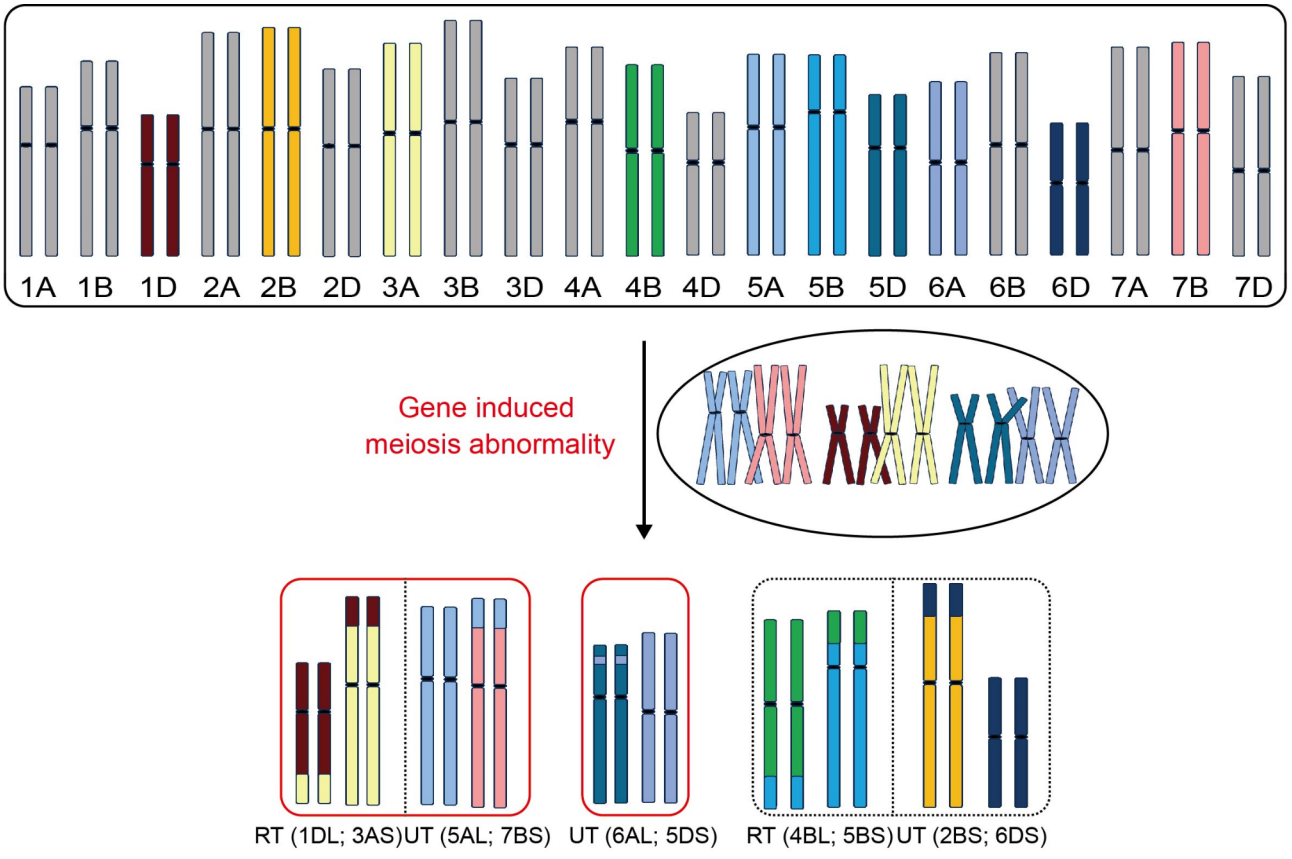

Fig. 6 Schematic illustration of the putative mechanism responsible for CSVs in *ds1*. The red rounded rectangles include the existed chromosome structural variations in the progenies of *ds1*. The rectangle with dotted lines indicted the possible chromosome structural variations in the progenies of *ds1*. CSVs, chromosome structural variations

the chromosome structure may not be stable in the early generation of *ds1*, and the progeny lines from *ds1* may still carry other chromosome translocations. It is worthwhile to further detect the chromosome structure of offsprings derived from *ds1* to identify new CSVs and evaluate the phenotypic effects, to provides potential genetic resources for future wheat improvement.

The spike morphology variation of *ds1* was attributed to the UT (5AL; 7BS)

Wheat spike architecture plays an important role in determining the grain number and size, which is a significant trait for improving yield [55]. Here, we identified an EMS-induced wheat mutant, *ds1*, which presented a compact spike and dwarf phenotype (Fig. 1). By combining BSA-Seq analysis and genetic mapping, the candidate gene was ultimately located on the partial unidirectional translocation from 5AL to 7BS chromosome, which resulted in the increasing *Q* gene copy number and expression (Fig. 4c).

The wheat domestication gene *Q* encodes an APETALA2-like transcription factor (TF) that plays pleiotropic roles in many agronomic traits, such as plant height, spike morphology, threshability and heading time [9, 14]. To determine whether the *Q* gene controls the spike morphology variation in *ds1*, the copy number variation and transcript level of the *Q* gene in *ds1* were examined. In addition, we sequenced the *Q* gene with specific primers to exclude potential mutations within *Q*. However, we did not find any difference within the sequence of the *Q* gene amplified from *ds1* or ND3753 (Fig. S4). Consequently, the results demostrated that an elevated expression level of *Q* in *ds1* compared to ND3753 was a contributing factor for the dense spike phenotype, which exhibited similarities to that of tetrasomic 5A plants, confirming the dosage effects of *Q* gene on spike morphology [7, 49].

The role of chromosome structural variations in wheat

Chromosome structural variations have been observed frequently in different wheat species and have vital effects on phenotypic variation during wheat evolution and improvement. The typical chromosome rearrangements involving 4A, 5A, and 7B in wheat evolution have been illustrated by genetic and macrocollinearity analysis [21, 56]. In the new synthetic hexaploid, the chromosomes seem to be unstable since the telosomes, deletions, and translocations are usually found in synthetic hexaploid wheat (SHW). Chromosomes 1B, 4D, 1D, 4B, and 5A have been reported to show more variations [57]. Combined with the observations of UT (5AL; 7BS) in this study, chromosomes 7B and 5A seem to be more active and easier to transform. There might be some specific sequences or structures on 7B and 5A that are more prone to vary and need further study. Unlike the UT, RT (1DL; 3AS) leads to chromosome rearrangement without large fragment losses or duplicates on chromosomes, which may have some positive effects on wheat agronomic traits. The polymorphic CRs were reported to be linked to plant ecological adaptation and crop improvement [58, 59]. Therefore, the RT (1DL; 3AS) found in *ds1* could be used for wheat breeding, such as 5BS•7BS/5BL•7BL in 66% of the 538 United Kingdom wheat lines [18, 22].

However, chromosome translocations, inversions and deletions can affect homologous recombination and exchange the gene order at the break points, which are significant barriers to positional cloning. Here, we crossed *ds1* with the parental line ND3753, followed by the selfing of F_1 individuals to generate F_2 progenies. Using BSA-Seq, we identified the candidate genes located on chromosome 7B. We developed the single nucleotide polymorphism variations between *ds1* and ND3753 as KASP (Kompetitive Allele-Specific PCR) markers to facilitate the mapping of candidate genes. However, the KASP markers located on 0-135 Mb of 7BS were difficult to design and were unstable during the genotyping assay. Therefore, we used an additional population of *ds1*×Y3002 for map-based cloning, which can easily design markers to identify the genotypes of progenies since the abundant genetic variations between *ds1* and Y3002. On the basis of next-generation sequencing and reads counts analysis, the present and absent structural variations, duplicate variations, and introgressions can be identified, which can provide useful information. We suggest that before mapping, the chromosome structure should be considered first, as several chromosome translocations have been reported in many founder wheat lines and 39.7% of 373 Chinese cultivars [23, 25].

Conclusion

This study identified an EMS-induced dense spike mutant, *dense spike1* (*ds1*), with dwarf plants and increased spike density. By combining map-based cloning, sequence comparison, and cytological and expression analyses, partial unidirectional translocation from 5AL to 7BS was identified in *ds1*. This UT (5AL; 7BS) resulting in an increase in the copy number and expression of *Q* gene, which is one of the reasons for the dense spike phenotype. Overall, we detected a partial unidirectional translocation from 5AL to 7BS as well as other chromosome structure variations in the EMS mutant population, which provides potential genetic resources for future wheat improvement.

Supplementary Information

The online version contains supplementary material available at https://doi.org/10.1186/s12864-024-11000-y.

Supplementary Material 1

Supplementary Material 2

Acknowledgements
We thank Zhen Qin, Zhengzhao Yang, Xiaoming Xie and Wenxi Wang from China Agricultural University for technical support. We appreciate Mingshan You from China Agricultural University for providing the mutant material *ds1*.

Author contributions
H.P. and M.H. supervised this work. H.P., M.H., Z.N., and Q.S. conceived this work. X.Z., Y.W., P.G., and Y.C. performed analyses. X.Z., Y.L., K.G., and J.X. performed experiments. X.Z., Y.W., Y.C., M.X., Z.H., W.G., Y.Y., Z.N., Q.S., M.H., and H.P. interpreted data. X.Z., T.L., and Y.W. wrote the manuscript, and M.H. and H.P. revised it. All authors read and approved the final manuscript.

Funding
This work was supported by grants from the National Natural Science Foundation of China (31991210), the Joint Research Program for Breeding of Inner Mongolia Autonomous Region, China (YZ2023008), and the Scientific and Technological Innovation 2030 Major Project (2023ZD0402301).

Data availability
The raw sequence data of two BSA-Seq analysis generated in this study have been deposited in the Sequence Read Archive under the accession code PRJNA1133897.

Declarations

Ethics approval and consent to participate
No specific permit is required for the samples in this study. We comply with relevant institutional, national, and international guidelines and legislation for plant studies.

Consent for publication
Not applicable.

Competing interests
The authors declare no competing interests.

Received: 17 August 2024 / Accepted: 5 November 2024
Published online: 12 November 2024

References

1. Zorb C, Ludewig U, Hawkesford MJ. Perspective on wheat yield and quality with reduced nitrogen supply. Trends Plant Sci. 2018;23(11):1029–37.
2. Jost M, Taketa S, Mascher M, Himmelbach A, Yuo T, Shahinnia F, et al. A homolog of blade-on-petiole 1 and 2 (*BOP1/2*) controls internode length and homeotic changes of the barley inflorescence. Plant Physiol. 2016;171(2):1113–27.
3. Konopatskaia I, Vavilova V, Blinov AG, Goncharov NP. Spike morphology genes in wheat species (*Triticum* L.). Proceedings of LAS. Section B. Natural, Exact, and Applied Sciences. 2016;70:345–355.
4. Kajla A, Schoen A, Paulson C, Yadav IS, Neelam K, Riera-Lizarazu O, et al. Physical mapping of the wheat genes in low-recombination regions: radiation hybrid mapping of the C-locus. Theor Appl Genet. 2023;136(7):159.
5. Johnson EB, Nalam VJ, Zemetra RS, Riera-Lizarazu O. Mapping the compactum locus in wheat (*Triticum aestivum* L.) and its relationship to other spike morphology genes of the *Triticeae*. Euphytica. 2008;163(2):193–201.
6. PrabhakaraRao MV. Mapping of the compactum gene C on chromosome 2D of wheat. Wheat Inform Service. 1972;35:9.
7. Muramatsu M. Dosage effect of the spelta gene *q* of hexaploid wheat. Genetics. 1963;48(4):469–82.
8. Muramatsu M. The vulgare super gene, *Q*: its universality in durum wheat and its phenotypic effects in tetraploid and hexaploid wheats. Can J Genet Cytol. 1986;28(1):30–41.
9. Faris JD, Gill BS. Genomic targeting and high-resolution mapping of the domestication gene *Q* in wheat. Genome. 2002;45(4):706–18.
10. Faris JD, Fellers JP, Brooks SA, Gill BS. A bacterial artificial chromosome contig spanning the major domestication locus *Q* in wheat and identification of a candidate gene. Genetics. 2003;164(1):311–21.
11. Kato K, Sonokawa R, Miura H, Sawada S. Dwarfing effect associated with the threshability gene *Q* on wheat chromosome 5A. Plant Breed. 2003;122(6):489–92.
12. Zhang Z, Belcram H, Gornicki P, Charles M, Just J, Huneau C, et al. Duplication and partitioning in evolution and function of homoeologous *Q* loci governing domestication characters in polyploid wheat. Proc Natl Acad Sci. 2011;108(46):18737–42.
13. Sormacheva I, Golovnina K, Vavilova V, Kosuge K, Watanabe N, Blinov A, et al. *Q* gene variability in wheat species with different spike morphology. Genet Resour Crop Ev. 2015; 62(6):837–852.
14. Simons KJ, Fellers JP, Trick HN, Zhang Z, Tai Y, Gill BS, et al. Molecular characterization of the major wheat domestication gene *Q*. Genetics. 2006;172(1):547–55.
15. Greenwood JR, Finnegan EJ, Watanabe N, Trevaskis B, Swain SM. New alleles of the wheat domestication gene *Q* reveal multiple roles in growth and reproductive development. Development. 2017;144(11):1959–65.
16. Debernardi JM, Lin H, Faris JD, Dubcovsky J. microRNA172 plays a critical role in wheat spike morphology and grain threshability. Development (Cambridge). 2017.
17. Schiessl S, Katche E, Ihien E, Chawla HS, Mason AS. The role of genomic structural variation in the genetic improvement of polyploid crops. Crop J. 2019;7(2):127–40.
18. Lv R, Gou X, Li N, Zhang Z, Wang C, Wang R, et al. Chromosome translocation affects multiple phenotypes, causes genome-wide dysregulation of gene expression, and remodels metabolome in hexaploid wheat. Plant J. 2023;115(6):1564–82.
19. Nicolas SD, Mignon GL, Eber F, Coriton O, Monod H, Clouet V, et al. Homeologous recombination plays a major role in chromosome rearrangements that occur during meiosis of *Brassica napus* haploids. Genetics. 2007;175(2):487–503.
20. Faria R, Johannesson K, Butlin RK, Westram AM. Evolving inversions. Trends Ecol Evol. 2019;34(3):239–48.
21. Dvorak J, Wang L, Zhu T, Jorgensen CM, Luo MC, Deal KR, et al. Reassessment of the evolution of wheat chromosomes 4A, 5A, and 7B. Theor Appl Genet. 2018;131(11):2451–62.
22. Walkowiak S, Gao L, Monat C, Haberer G, Kassa MT, Brinton J, et al. Multiple wheat genomes reveal global variation in modern breeding. Nature. 2020;588(7837):277–83.
23. Huang X, Zhu M, Zhuang L, Zhang S, Wang J, Chen X, et al. Structural chromosome rearrangements and polymorphisms identified in Chinese wheat cultivars by high-resolution multiplex oligonucleotide FISH. Theor Appl Genet. 2018;131(9):1967–86.
24. Zhao J, Zheng X, Qiao L, Yang C, Wu B, He Z, et al. Genome-wide association study reveals structural chromosome variations with phenotypic effects in wheat (*Triticum aestivum* L). Plant J. 2022;112(6):1447–61.
25. Wu N, Lei Y, Pei D, Wu H, Liu X, Fang J, et al. Predominant wheat-alien chromosome translocations in newly developed wheat of China. Mol Breed. 2021;41(4).
26. Liu C, Ye X, Wang M, Li S, Lin Z. Genetic behavior of *Triticum aestivum-Dasypyrum villosum* translocation chromosomes T6V#4S·6DL and T6V#2S·6AL carrying powdery mildew resistance. J Integr Agric. 2017;16:2136–44.
27. Schlegel R, Korzun V. About the origin of 1RS.1BL wheat-rye chromosome translocations from Germany. Plant Breed. 1997;116(6):537–40.
28. Naseeb S, Carter Z, Minnis D, Donaldson I, Zeef L, Delneri D. Widespread impact of chromosomal inversions on gene expression uncovers robustness via phenotypic buffering. Mol Biol Evol. 2016;33(7):1679–96.
29. Wesley CS, Eanes WF. Isolation and analysis of the breakpoint sequences of chromosome inversion *In(3L)Payne* in *Drosophila melanogaster*. Proc Natl Acad Sci. 1994;91(8):3132–3136.
30. Chen S, Zhou Y, Chen Y, Gu J. Fastp: an ultra-fast all-in-one FASTQ preprocessor. Bioinformatics. 2018;34(17):i884–90.
31. International Wheat Genome Sequencing (IWGSC), Appels R, Eversole K, Stein N, Feuillet C, Keller B, et al. Shifting the limits in wheat research and breeding using a fully annotated reference genome. Science. 2018;361(6403):r7191.
32. Zhu T, Wang L, Rimbert H, Rodriguez JC, Deal KR, De Oliveira R, et al. Optical maps refine the bread wheat *Triticum aestivum* Cv. Chinese spring genome assembly. Plant J. 2021;107(1):303–14.
33. Li H, Durbin R. Fast and accurate short read alignment with Burrows–Wheeler transform. Bioinformatics. 2009;25(14):1754–60.

34. McKenna A, Hanna M, Banks E, Sivachenko A, Cibulskis K, Kernytsky A, et al. The genome analysis Toolkit: a MapReduce framework for analyzing next-generation DNA sequencing data. Genome Res. 2010;20(9):1297–303.
35. Danecek P, Auton A, Abecasis G, Albers CA, Banks E, DePristo MA, et al. The variant call format and VCFtools. Bioinformatics. 2011;27(15):2156–8.
36. Cingolani P, Platts A, Wang LL, Coon M, Nguyen T, Wang L, et al. A program for annotating and predicting the effects of single nucleotide polymorphisms, SnpEff. Fly. 2012;6(2):80–92.
37. Mesapogu S, Jillepalli CM, Arora DK. Agarose gel electrophoresis and polyacrylamide gel electrophoresis: Methods and Principles. In: Analyzing Microbes: Manual of Molecular Biology Techniques. Edited by Arora DK, Das S, Sukumar M. Berlin, Heidelberg: Springer Berlin Heidelberg; 2013: 73–91.
38. Porebski S, Bailey LG, Baum BR. Modification of a CTAB DNA extraction protocol for plants containing high polysaccharide and polyphenol components. Plant Mol Biol Rep. 1997;15(1):8–15.
39. Ma S, Wang M, Wu J, Guo W, Chen Y, Li G, et al. WheatOmics: a platform combining multiple omics data to accelerate functional genomics studies in wheat. Mol Plant. 2021;14(12):1965–8.
40. Waddington SR, Cartwright PM, Wall PC. A quantitative scale of spike initial and pistil development in barley and wheat. Ann Bot. 1983;51(1):119–30.
41. Livak KJ, Schmittgen TD. Analysis of relative gene expression data using real-time quantitative PCR and the $2^{-\Delta\Delta CT}$ method. Methods. 2001;25(4):402–8.
42. Tang S, Tang Z, Qiu L, Yang Z, Li G, Lang T, et al. Developing new oligo probes to distinguish specific chromosomal segments and the A, B, D genomes of wheat (*Triticum aestivum* L.) using ND-FISH. Front Plant Sci. 2018;9.
43. Tang Z, Yang Z, Fu S. Oligonucleotides replacing the roles of repetitive sequences pAs1, pSc119.2, pTa-535, pTa71, CCS1, and pAWRC.1 for FISH analysis. J Appl Genet. 2014;55(3):313–8.
44. Han F, Liu B, Fedak G, Liu Z. Genomic constitution and variation in five partial amphiploids of wheat-*Thinopyrum* intermedium as revealed by GISH, Multicolor GISH and seed storage protein analysis. Theor Appl Genet. 2004;109(5):1070–6.
45. Díaz A, Zikhali M, Turner AS, Isaac P, Laurie DA. Copy number variation affecting the photoperiod-B1 and vernalization-A1 genes is associated with altered flowering time in wheat (*Triticum aestivum*). PLoS ONE. 2012;7(3):e33234.
46. Nemoto Y, Kisaka M, Fuse T, Yano M, Ogihara Y. Characterization and functional analysis of three wheat genes with homology to the *CONSTANS* flowering time gene in transgenic rice. Plant J. 2003;36(1):82–93.
47. Trick M, Adamski NM, Mugford SG, Jiang C, Febrer M, Uauy C. Combining SNP discovery from next-generation sequencing data with bulked segregant analysis (BSA) to fine-map genes in polyploid wheat. BMC Plant Biol. 2012;12(1):14.
48. Förster S, Schumann E, Eberhard Weber W, Pillen K. Discrimination of alleles and copy numbers at the *Q* locus in hexaploid wheat using quantitative pyrosequencing. Euphytica. 2012;186(1):207–18.
49. Förster S, Schumann E, Baumann M, Weber WE, Pillen K. Copy number variation of chromosome 5A and its association with *Q* gene expression, morphological aberrations, and agronomic performance of winter wheat cultivars. Theor Appl Genet. 2013;126(12):3049–63.
50. Kim Y, Schumaker KS, Zhu J. EMS mutagenesis of *Arabidopsis*. In: Salinas J, Sanchez-Serrano JJ. Totowa, NJ, editors. *Arabidopsis* Protocols. Humana Press; 2006. p. 101–103.
51. Türkoğlu A, Haliloğlu K, Tosun M, Bujak H, Eren B, Demirel F, et al. Ethyl Methanesulfonate (EMS) mutagen toxicity-induced DNA damage, cytosine methylation alteration, and iPBS-retrotransposon polymorphisms in wheat (*Triticum aestivum* L.). In: Agronomy., vol. 13;2023.
52. Gnanamurthy S, Dhanavel D. Effect of EMS on induced morphological mutants and chromosomal variation in cowpea (*Vigna unguiculata* (L.) Walp). Int Lett Nat Sci. 2014;22:33–43.
53. Wu L, Li G, Li D, Dong C, Zhang X, Zhang L, et al. Identification and functional analysis of a chromosome 2D fragment harboring *TaFPF1* gene with the potential for yield improvement using a late heading wheat mutant. Theor Appl Genet. 2024;137(4):92.
54. Wang D, Li Y, Wang H, Xu Y, Yang Y, Zhou Y, et al. Boosting wheat functional genomics via an indexed EMS mutant library of KN9204. Plant Commun. 2023;4(4):100593.
55. Cao S, Xu D, Hanif M, Xia X, He Z. Genetic architecture underpinning yield component traits in wheat. Theor Appl Genet. 2020;133(6):1811–23.
56. Chen Y, Song W, Xie X, Wang Z, Guan P, Peng H, et al. A collinearity-incorporating homology inference strategy for connecting emerging assemblies in the *Triticeae* tribe as a pilot practice in the plant pangenomic era. Mol Plant. 2020;13(12):1694–708.
57. Zhang S, Du P, Lu X, Fang J, Wang J, Chen X, et al. Frequent numerical and structural chromosome changes in early generations of synthetic hexaploid wheat. Genome. 2021;65(4):205–17.
58. Todesco M, Owens GL, Bercovich N, Légaré J, Soudi S, Burge DO, et al. Massive haplotypes underlie ecotypic differentiation in sunflowers. Nature. 2020;584(7822):602–7.
59. Martin G, Baurens F, Hervouet C, Salmon F, Delos J, Labadie K, et al. Chromosome reciprocal translocations have accompanied subspecies evolution in bananas. Plant J. 2020;104(6):1698–711.

Publisher's note